

# Proton radius reconstruction from the pseudo-data on electron-proton elastic scattering at low transfer momenta

S.Belostotski, N.Sagidova, A.Vorobyev

*Petersburg Nuclear Physics Institute*

*NRC "Kurchatov Institute", Gatchina, Russia*

Contact person : Alexey Vorobyev

email : vorobyov\_aa@pnpi.nrcki.ru

December 15, 2024

## Abstract

This note is motivated by preparations of a new  $ep$  elastic scattering experiment in the low transfer momentum region to be carried out in the 720 MeV electron beam of the Mainz Microtron MAMI. This experiment will use an innovative method allowing for detection of recoil protons in coincidence with the scattered electrons. The goal is to measure the  $ep$  differential cross sections in the  $Q^2$  range from 0.001 GeV<sup>2</sup> to 0.04 GeV<sup>2</sup> and to determine the proton charge radius with sub-percent precision.

In the  $ep$  elastic scattering experiments, the proton charge radius is extracted from the slope of the electric form factor at the momentum transfer squared  $Q^2 > 0$ . In order to estimate the level of statistical and systematic errors in the extracted proton radius, we simulated the  $ep$  elastic scattering differential cross section using the proton form factor available from analysis of the experimental data from the A1 experiment at Mainz. Then the proton radius was extracted from fitting the simulated pseudo-data with the cross section calculated using a  $Q^2$  power series expansion of the proton electric form factor up to the  $Q^8$  term. About 70 million of the  $ep$  elastic scattering events were generated in the  $Q^2$  range from 0.001 GeV<sup>2</sup> to 0.04 GeV<sup>2</sup>, that corresponds to the statistics to be collected in our experiment in 45 days. For the considered  $Q^2$  range and statistics, the main conclusions of these studies are as follows:

- The extracted value of the proton charge radius is not sensitive to the  $Q^8$  term, so this term can be neglected in the fits.
- The fits with four free parameters ( $A, < r_p^2 >, < r_p^4 >, < r_p^6 >$ ) determine the proton charge *rms*-radius  $R_p = < r_p^2 >^{1/2}$  with the errors  $\Delta R_p(\text{stat}) = 0.0085$  fm (sigma) and  $\Delta R_p(\text{syst}) \leq 0.001$  fm.
- The statistical error can be reduced by a factor of two down to  $\Delta R_p(\text{stat}) = 0.0042$  fm by fixing parameter  $< r_p^6 >$  to some value determined in the experiments performed at larger transfer momenta. As an example, we have used the published value of  $< r_p^6 > = 29.8$  (7.6)(12.6) fm<sup>6</sup> determined in such experiments. Unfortunately, this value suffers from rather large systematic uncertainty that resulted in a systematic error in the extracted proton radius :  $\Delta R_p(\text{syst}) = 0.0025$  fm. Another promising approach, discussed in this note, is to use a theoretical value for  $< r_p^6 >$  in the fits .

# 1 Introduction

The striking difference in the proton charge *rms*-radius extracted from the two types of experiments, the elastic  $ep$  scattering experiments (  $R_p = 0.879$  (5)(6) fm [1] ) and the muonic Lamb shift experiments (  $R_p = 0.8409$  (4) fm [2] ), so called “proton radius puzzle”, is widely discussed, *see e.g.* [3]. As it is generally agreed, new high precision measurements of the  $ep$  scattering differential cross sections in the low momentum transfer region are needed to resolve this puzzle. Recently, a new experiment was proposed by our collaboration [4] to be carried out in the 720 MeV electron beam of the Mainz Microtron MAMI. An innovative method will be used allowing for detection of recoil protons in coincidence with the scattered electrons. The goal of this experiment is to measure the  $ep$  differential cross sections in the  $Q^2$  range from 0.001 GeV<sup>2</sup> to 0.04 GeV<sup>2</sup> with 0.1 % relative and 0.2% absolute precision and to determine the proton charge radius with sub-percent precision. In this  $Q^2$  range, about 70 million  $ep$  elastic scattering events should be collected in 45 days of the beam time.

This note considers possible algorithms of analysis of the experimental data from this experiment. In order to estimate the level of statistical and systematic errors in the extracted proton radius, we simulated the  $ep$  elastic scattering differential cross section using the proton form factor available from analysis of the experimental data from the A1 experiment at Mainz. Then the proton radius was extracted from fitting the simulated pseudo-data with the cross section calculated using various approximations for the  $Q^2$  dependence of the proton form factor.

## 2 Generation of $ep$ scattering events

For this analysis, the  $ep$  scattering events were generated according to the following function describing the  $ep$  elastic scattering differential cross section:

$$\frac{d\sigma}{dt} = \frac{\pi\alpha^2}{t^2} \left\{ G_E^2 \left[ \frac{(4M + t/\varepsilon_e)^2}{4M^2 - t} + \frac{t}{\varepsilon_e^2} \right] - \frac{t}{4M^2} G_M^2 \left[ \frac{(4M + t/\varepsilon_e)^2}{4M^2 - t} - \frac{t}{\varepsilon_e^2} \right] \right\} \text{GeV}^{-4} \quad (1)$$

where  $-t = Q^2$ ;  $\alpha = 1/137.036$ ;  $M$  is the proton mass ( $M = 938.272$  MeV);  $\varepsilon_e$  is the total electron energy ( $\varepsilon_e = 720.5$  MeV);  $G_E(Q^2)$  and  $G_M(Q^2)$  are the electric and magnetic form factors, respectively. We have accepted the following approximation valid for the small  $Q^2$  region:

$$G_M(Q^2) = \mu_p \cdot G_E(Q^2) = 2.793 G_E(Q^2) \quad (2)$$

$G_E(Q^2)$  is taken as a power series expansion:

$$G_E(Q^2) = 1 - R_2 \cdot B_2 \cdot Q^2 / C_2 + R_4 \cdot B_4 \cdot Q^4 / C_4 - R_6 \cdot B_6 \cdot Q^6 / C_6 + R_8 \cdot B_8 \cdot Q^8 / C_8 \quad (3)$$

where  $B_n = (5.06773)^n$ ,  $C_n = (n+1)!$ ,  $n=2,4,6,8$ ;  $R_2 = \langle r_p^2 \rangle$ ,  $R_4 = \langle r_p^4 \rangle$ ,  $R_6 = \langle r_p^6 \rangle$ , and  $R_8 = \langle r_p^8 \rangle$ . The *rms*-radius  $R_p = (R_2)^{1/2}$ . In such presentation,  $\langle r_p^n \rangle$  and  $Q^n$  are expressed in  $\text{fm}^n$  and in  $\text{GeV}^n$ , respectively.

1 fm = 5.06773 GeV<sup>-1</sup>; 1 GeV<sup>-2</sup> = 0.389379 mb. The  $ep$  scattering events were generated in the  $Q^2$  range from 0.001 GeV<sup>2</sup> to 0.04 GeV<sup>2</sup> using the values of  $R_2$ ,  $R_4$ ,  $R_6$ , and  $R_8$  obtained by J.C.Bernauer [5,6] from analysis of the cross sections measured in the A1 experiment:

$$R_2 = 0.7700 \text{ fm}^2, R_4 = 2.63 \text{ fm}^4, R_6 = 26 \text{ fm}^6, R_8 = 374 \text{ fm}^8.$$

The corresponding proton *rms*-radius is  $R_p = (R_2)^{1/2} = (0.7700 \text{ fm}^2)^{1/2} = 0.8775 \text{ fm}$ .

The *ep* scattering cross sections integrated over the  $Q^2$  range  $0.001 \text{ GeV}^2 \leq Q^2 \leq 0.04 \text{ GeV}^2$  are:  $\sigma(R_p = 0.8775 \text{ fm}) = 0.248703 \text{ mb}$  and  $\sigma(R_p = 0) = 0.254724 \text{ mb}$ .

The ratio of these cross sections is  $K = 0.976363$ .

As it follows from eqs.(1) and (2), the ratio of the differential cross sections gives the form factor squared in function of  $Q^2$ :

$$d\sigma/dt(R_p = 0.8775 \text{ fm})/d\sigma/dt(R_p = 0) = G_E^2(Q^2). \quad (4)$$

We find this ratio by generating two similar samples of the *ep* scattering events: one for  $R_p = 0.8775 \text{ fm}$  and another one for  $R_p = 0$ . These samples should correspond to the same luminosity. That means that the number of generated events for  $R_p = 0.8775 \text{ fm}$  should be by a factor of  $K = 0.976363$  less than that for  $R_p = 0$ . Then the value of  $(G_E)_i^2$  in each bin can be obtained by the ratio of the numbers of generated events in that bin.

$$(G_E)_i^2 = N_i(R_p = 0.8775 \text{ fm})/N_i(R_p = 0) \quad (5)$$

In order to reduce contribution of fluctuations in  $N_i(R_p=0)$  to the statistical error in  $(G_E)_i^2$ , the  $(R_p=0)$  sample is generated with 100 times larger statistics, therefore eq. (5) is transformed to:

$$(G_E)_i^2 = N_i(R_p = 0.8775 \text{ fm})/0.01 N_i(R_p = 0). \quad (6)$$

The *ep* scattering events were generated using the ROOT framework. ROOT is a modular scientific software toolkit, it provides all the functionalities needed to deal with data processing, simulation, statistical analysis, visualisation, and storage. Besides the analytical function of  $d\sigma/dt$ , this program required as the input parameters: the  $Q^2$  range, the binning within this range, and the total number of generated events. At the level of the events generation, we use 1000 bins of equal width in the  $Q^2$  range  $0.001 \text{ GeV}^2 \leq Q^2 \leq 0.04 \text{ GeV}^2$  with a possibility of further re-binning of the generated  $G_E^2(Q^2)$  distribution. For each bin, the program gives the numbers of events integrated over the bin width,  $N_i(R_p = 0.8775 \text{ fm})$  and  $N_i(R_p = 0)$ , and determines  $(G_E)_i^2$  according to eq.(6). About 70 million events generated in the  $Q^2$  range from  $0.001 \text{ GeV}^2$  to  $Q^2 = 0.04 \text{ GeV}^2$  correspond to the expected number of events to be collected in our experiment in 45 days of continuous running with integrated luminosity  $L_{int} = 2.8 \cdot 10^8 \text{ mb}^{-1}$ . As an example, Figure 1 presents the simulated differential cross sections. The total number of generated events was  $N_{ev}(R_p = 0.8775 \text{ fm}) = 6.96369 \cdot 10^7$  events and  $N_{ev}(R_p = 0) = 7.13227 \cdot 10^9$  events. Figure 2 (left panel) shows the  $G_E^2(Q^2)$  distribution determined according to eq.(6). The right panel shows the same spectrum after re-binning the generated spectrum to 100 bins in the same  $Q^2$  range.

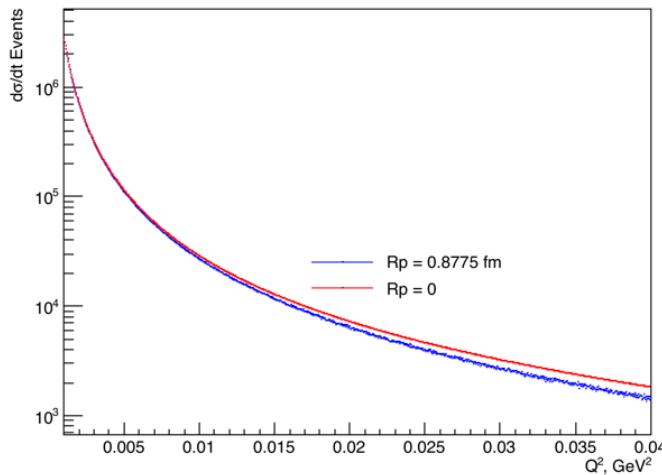


**Figure 1:** Simulated differential cross sections for  $R_p=0.8775 \text{ fm}$  (blue line) and for  $R_p=0$  (red line). Statistics:  $N_{ev}(R_p=0.8775 \text{ fm}) = 6.96369 \cdot 10^7$  events.  $N_{ev}(R_p=0) = 7.13227 \cdot 10^9/100$  events. Binning: 1000 bins.

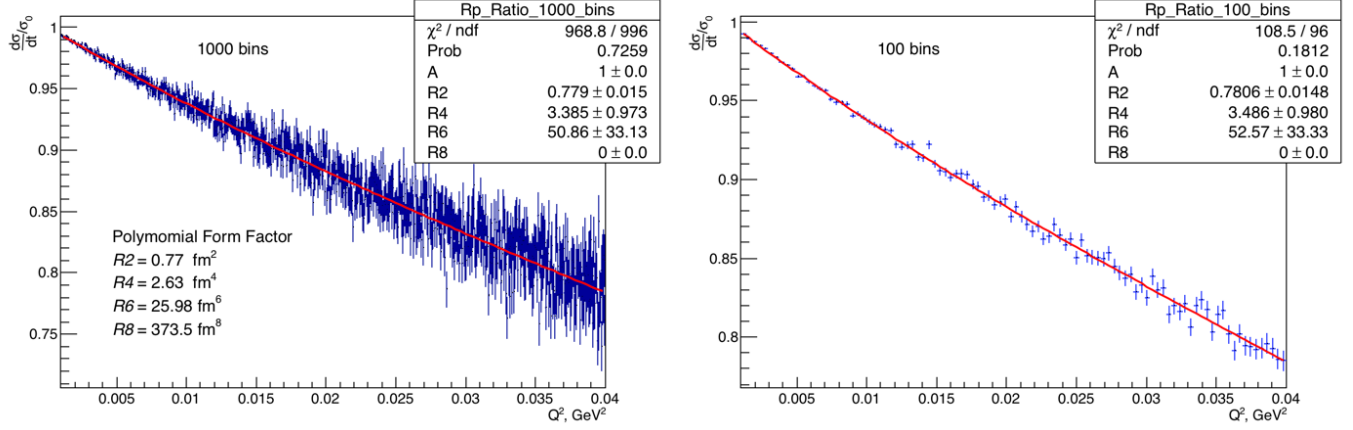


**Figure 2:** Distribution of the ratio of  $d\sigma/dt$  ( $R_p = 0.8775$  fm) /  $d\sigma/dt$  ( $R_p = 0$ ), equivalent to the  $G_E^2(Q^2)$  distribution, obtained according to eq.( 6). Statistics:  $N_{ev}(R_p = 0.8775 \text{ fm}) = 6.9636 \cdot 10^7$  events,  $N_{ev}(R_p = 0) = 7.13227 \cdot 10^9$  events. Binning: 1000 bins (left panel) and 100 bins (right panel). Red lines show the results of the fit with the form factor represented by Fit 1 in Table 1.

### 3 Fitting of the $G_E^2(Q^2)$ distributions

To fit the generated  $G_E^2(Q^2)$  distributions, we use the power series expansion of the form factor:

$$G_E(Q^2)_{fit} = A \cdot (1 - R_2 \cdot B_2 \cdot Q^2/C_2 + R_4 \cdot B_4 \cdot Q^4/C_4 - R_6 \cdot B_6 \cdot Q^6/C_6 + R_8 \cdot B_8 \cdot Q^8/C_8) \quad (7)$$

with the constants  $B_n$  and  $C_n$  as in eq.( 3). The goal was to see how many  $Q^2$  terms should be retained in this expression to provide minimal combined statistical plus systematic error in determination of the proton radius. The following options have been tested:

Option 1:  $A$ ,  $R_2$ ,  $R_4$ ,  $R_6$  are free parameters,  $R_8$  is a fixed variable.

Option 2:  $A$ ,  $R_2$ ,  $R_4$  are free parameters,  $R_6$  and  $R_8$  are fixed variables.

#### Statistical errors in measurements of the proton radius

Table 1 compares the statistical errors in  $R_2$  and  $R_4$  obtained by fitting the generated  $G_E^2(Q^2)$  with  $G_E(Q^2)_{fit}$  represented by eq.( 7) with four or three free parameters for statistics planned to collect in 45 days of continuous running of the experiment.

**Table 1:** Comparison of statistical errors in  $R_2$  and  $R_4$  in the fits with three and four free parameters.

FF\* denotes parameters used to generate the  $G_E^2(Q^2)$  distribution. Statistics:

$N_{ev}(R_p = 0.8775 \text{ fm}) = 6.9636 \cdot 10^7$  events,  $N_{ev}(R_p = 0) = 7.13227 \cdot 10^9$  events. Binning: 1000 bins.

	$R_2, fm^2$ $R_p, fm$	$R_4, fm^4$	$R_6, fm^6$	$R_8, fm^8$	$A$	$\chi^2 / \text{ndf}$
<b>FF*</b>	0.7700* 0.8775	2.63*	26*	374*		
<b>Fit 1</b>	0.7790 (150) 0.8826 (85)	$3.38 \pm 0.97$	$51 \pm 33$	<b>0 fixed</b>	1.0000(2)	969/996
<b>Fit 2</b>	0.7669 (72) 0.8757 (41)	$2.52 \pm 0.2$	<b>26 fixed</b>	<b>0 fixed</b>	0.9999 (2)	970/997

From comparison of Fit 1 and Fit 2 in Table 1, one can see that reduction of the number of free parameters *by fixing  $R6$  to some fixed value reduces the statistical error in determination of the proton radius by a factor of two* ( from  $\pm 0.0085$  fm to  $\pm 0.0041$  fm). Also, the  $R4$  parameter is determined with 8% precision in this fit.

### Systematic biases in measurement of the proton radius

We have performed a number of fitting sets with various fixed values of  $R6$  and  $R8$  to study possible systematic biases related to this procedure. In each fitting set the fit was repeated 1000 times with independently generated  $G_E^2(Q^2)$  distributions. Figures 3 and 4 show the examples of such fits with four free parameters and with three free parameters, respectively.

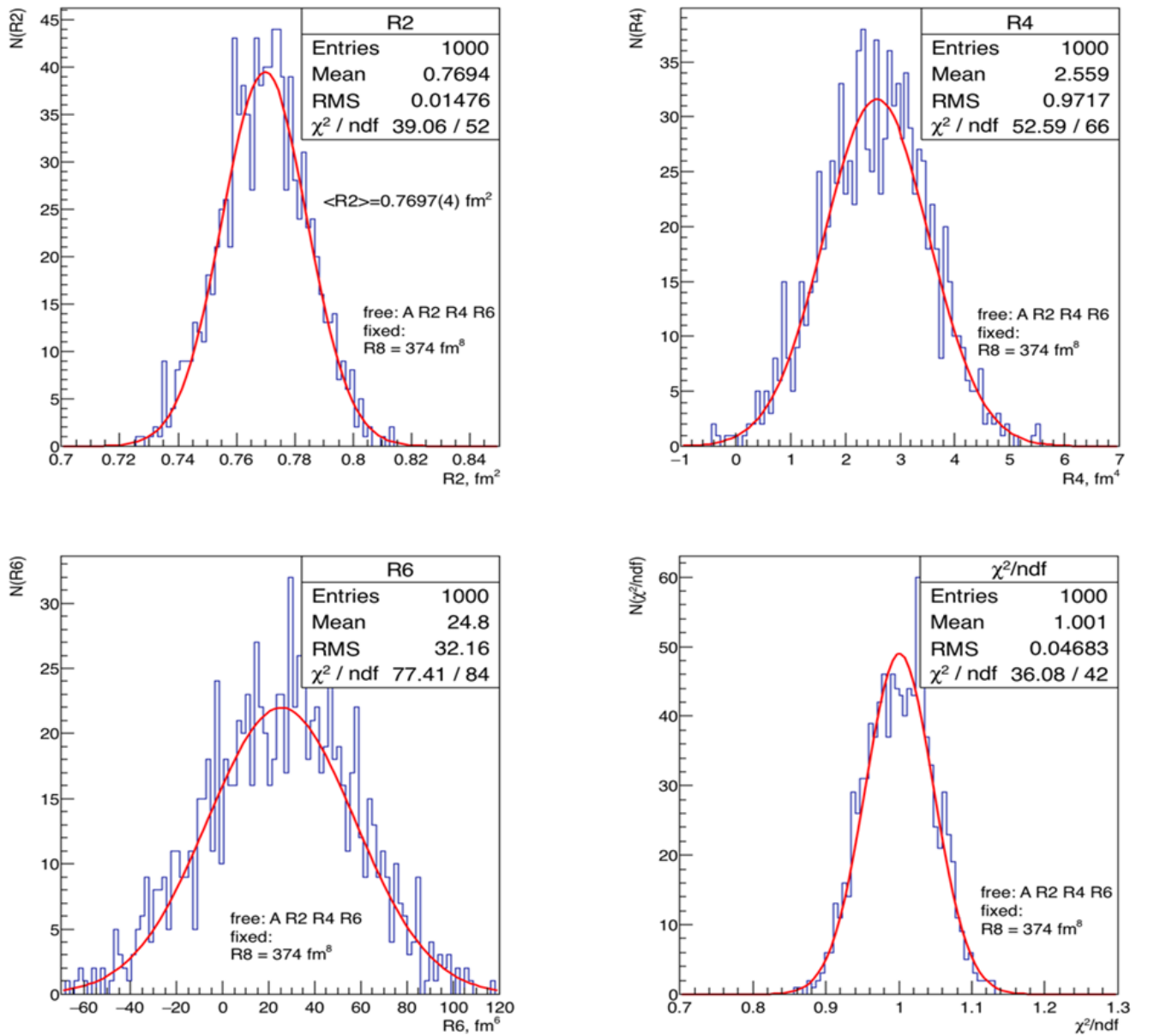


**Figure 3:** Distribution of the fitting parameters from the fits of 1000 independently generated  $G_E^2(Q^2)$  distributions. The fitting function contained four free parameters  $A, R2, R4, R6$  with  $R8 = 374 \text{ fm}^8$ .

Statistics:  $N_{ev}(R_p = 0.8775 \text{ fm}) = 6.9636 \cdot 10^7$  events in each  $G_E^2(Q^2)$  distribution. Binning: 1000 bins.

The distributions shown in Figs. 3, 4 were obtained with 1000 bins in the  $G_E^2(Q^2)$  distributions. The re-binning of these distributions to 100 bins gives identical fitting results, except the  $\chi^2$  distribution becomes wider by a factor of three (Fig. 5).

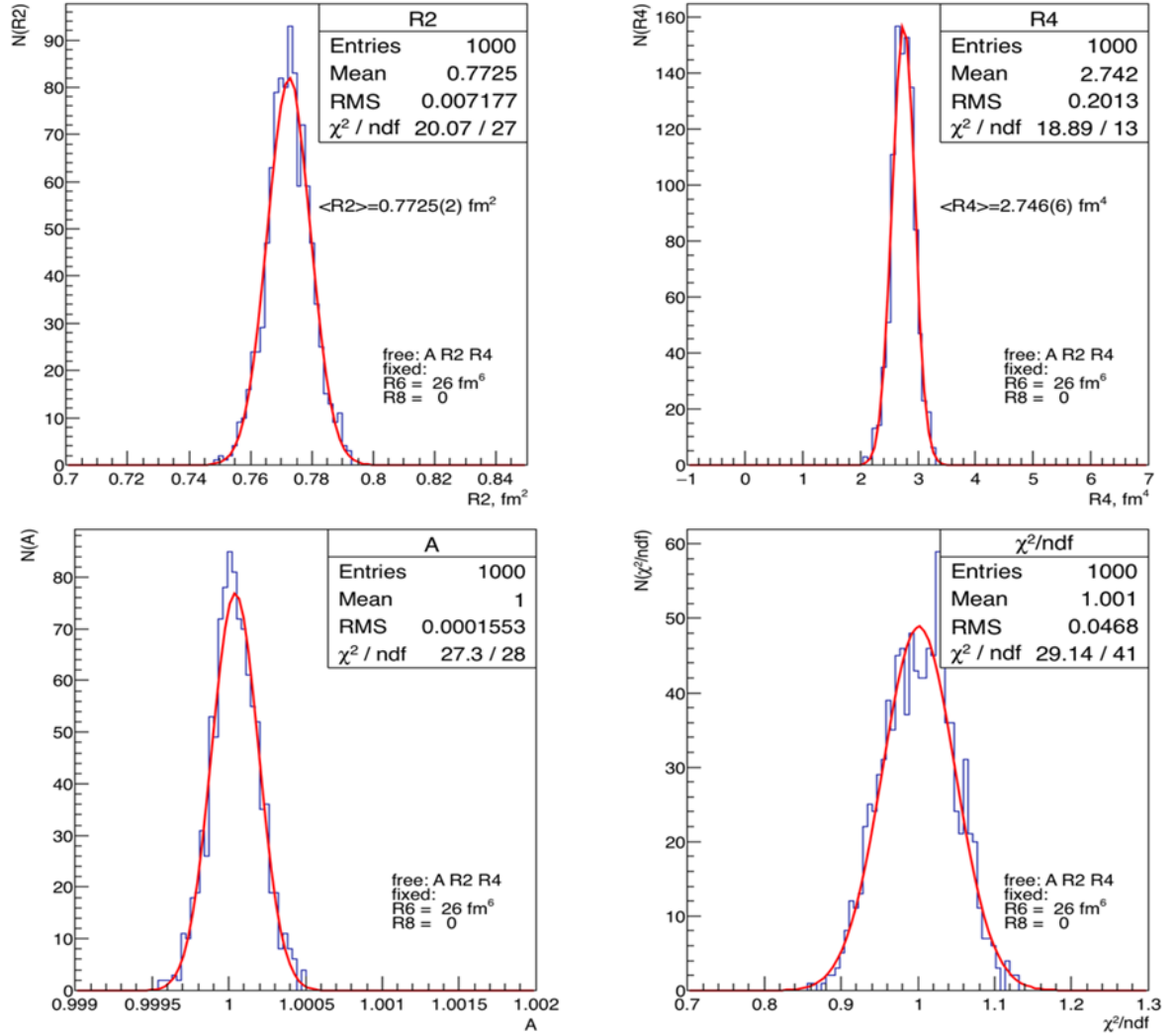


**Figure 4:** Distribution of the fitting parameters obtained in the fits of 1000 independently generated  $G_E^2(Q^2)$  distributions. The fitting function contained three free parameters  $A$ ,  $R2$ ,  $R4$ , with fixed  $R6 = 26 \text{ fm}^6$  and  $R8 = 0$ . Statistics:  $N_{ev}(R_p = 0.8775 \text{ fm}) = 6.9636 \cdot 10^7$  events in each  $G_E^2(Q^2)$  distribution. Binning: 1000 bins.

As it follows from Fig. 4, the fits with three free parameters can provide  $0.0072/0.770 = 0.94\%$  statistical precision in determination of  $R2$  (0.47% precision in  $R_p$ ). In addition,  $R4$  is measured with 8% statistical precision. In these fits,  $R6$  and  $R8$  were fixed to  $26 \text{ fm}^6$  and to zero, respectively. To see the sensitivity of obtained values of  $R2$  and  $R4$  to the chosen value of  $R6$ , the fits were repeated with  $R6 = 10 \text{ fm}^6$  and  $35 \text{ fm}^6$ . The results are presented in Figs. 6, 7 and in Table 2.

As concerns the influence of parameter  $R8$  on measurement of  $R2$ , it is proved to be practically negligible, as it follows from comparison of Fit1 with Fit2 in Table 2. The variation of  $R8$  from  $374 \text{ fm}^8$  to zero shifts the value of  $R2$  by 0.13% (0.065% shift in  $R_p$ ). On the other hand, the sensitivity of the extracted value of  $R2$  to the fixed values of  $R6$  is more essential (Fits 3,4,5). The variation of  $R6$  from  $10 \text{ fm}^6$  to  $35 \text{ fm}^6$  resulted in a systematic shifts of  $R2$  by 1.2 % (0.6% in  $R_p$ ).

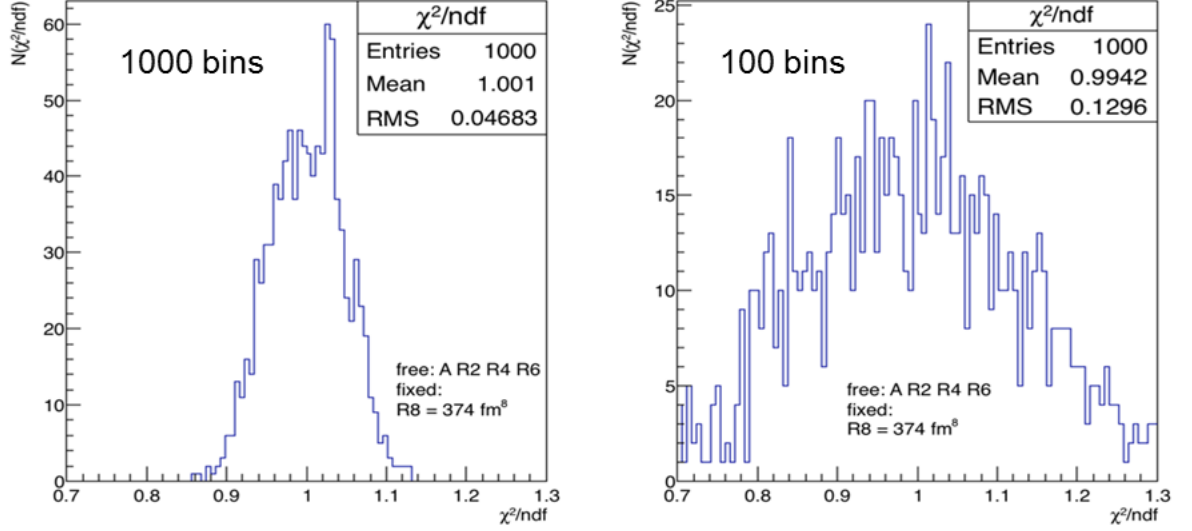


**Figure 5:** Comparison of  $\chi^2/\text{ndf}$  distributions obtained in fitting the same  $G_E^2(Q^2)$  distributions subdivided in 1000 bins (left panel) and in 100 bins (right panel)

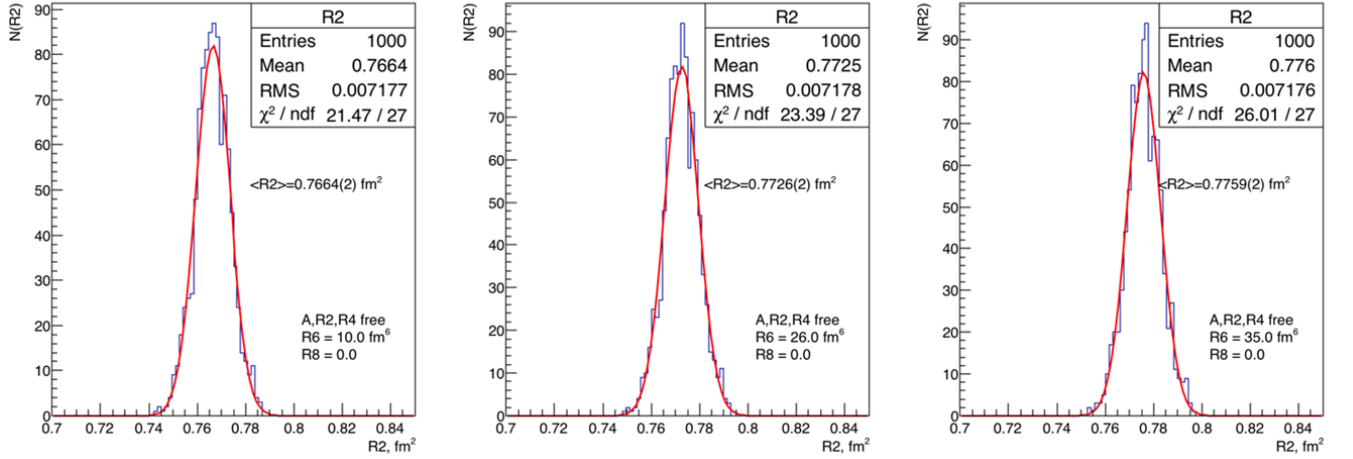


**Figure 6:** Dependence of the  $R2$  distributions on variation of the parameter  $R6$ :  $R6 = 10 \text{ fm}^6$  (left panel),  $26 \text{ fm}^6$  (central panel), and  $35 \text{ fm}^6$  (right panel).  $R8$  is set to zero. Red lines – fits with Gaussian distributions. The width of these distributions proved to be identical for all considered spectra.

The systematic biases were studied also by another method when the simulated cross sections were generated with 1000 times higher statistics: ( $N_{ev}(R_p = 0.8775 \text{ fm}) = 6.96369 \cdot 10^{10}$  events and  $N_{ev}(R_p = 0) = 7.13227 \cdot 10^{10}$  events). The results are presented in Table 3. As it follows from Fits 1,2,3 in Table 3, variation of  $R8$  from  $R8 = 0$  to  $R8 = 700 \text{ fm}^8$  resulted in a 0.2% shift in the extracted  $R2$  value. Therefore, it is safe to fix  $R8$  at  $R8 = 374 \text{ fm}^8$  and consider the systematic error in  $R2$  due to uncertainties in  $R8$  to be on a level of  $\pm 0.1 \%$  ( $0.05\%$  in  $R_p$ ).

While fixing the  $R6$  parameter, it is natural to take into account the results of previous analyses of the  $ep$  scattering data. According to [6],  $R6 = 29.8 (7.6)(12.6) \text{ fm}^6$  and  $R4 = 2.59 (19)(04) \text{ fm}^4$ . Therefore, we can fix  $R6$  at  $\approx 26 \text{ fm}^6$  with uncertainty of  $\pm 15 \text{ fm}^6$ . As one can see from Fits 4, 5, 6 in Table 3, such uncertainty in  $R6$  leads to  $\pm 0.8\%$  systematic errors in  $R2$  ( $\pm 0.4\%$  in  $R_p$ ).

As to the  $R4$  parameter, it can be determined directly from our experimental data, and comparison with the A1 data could be used as a cross check.



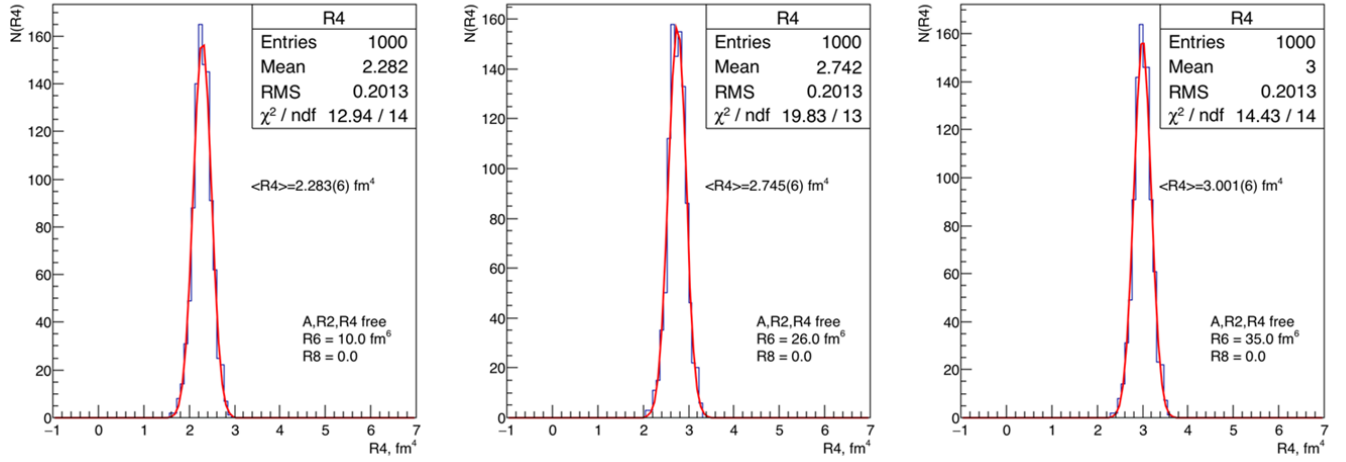


**Figure 7:** Dependence of the  $R4$  distributions on variation of the  $R6$  parameter :  $R6 = 10 \text{ fm}^6$  (left panel),  $26 \text{ fm}^6$  (central panel), and  $35 \text{ fm}^6$  (right panel).  $R8$  is set to zero.

**Table 2:** Mean values of the  $R2$  and  $R4$  parameters determined from the fits of 1000 independently generated  $G_E^2(Q^2)$  distributions (as shown in Fig. 2) for various options of the fixed parameters  $R6$  and  $R8$ . FF\* denotes the form factor parameters used to generate the  $G_E^2(Q^2)$  distribution. In all shown fits, the mean values of parameters  $A$  and  $\chi^2/\text{ndf}$  are equal to 1.0 with  $10^{-4}$  and  $10^{-3}$  accuracy, respectively.

Fit	$\langle R2 \rangle$ $\langle R2 \rangle - R2^*$ $\text{fm}^2$	$\langle R4 \rangle$ $\langle R4 \rangle - R4^*$ $\text{fm}^4$	$\langle R6 \rangle$ $\langle R6 \rangle - R6^*$ $\text{fm}^6$	$R8$ $\text{fm}^8$
FF*	0.7700*	2.63*	25.98*	373.5*
Fit1	0.7703(5) +0.0003(5)	2.61±0.03 -0.03(3)	26±1 0±1	374 fixed
Fit2	0.7693(5) -0.0007(5)	2.49±0.03 -0.14(3)	23.4±1.0 -1.6±1.0	0 fixed
Fit3	0.7727(2) +0.0027(2)	2.743(7) +0.113(7)	26 fixed	0 fixed
Fit4	0.7665(2) -0.0035(2)	2,284(7) -0.346(7)	10 fixed	0 fixed
Fit5	0.7761(2) +0.0061(2)	3.00(7) +0.37	35 fixed	0 fixed

Additional study of the systematic shifts in the  $R2$  values was done by fitting the ratio of the differential cross sections  $d\sigma/dt(R_p) / d\sigma/dt(R_p=0)$  generated with high statistics for three options of the polynomial Form Factor, FF1, FF2, and FF3, with variations of the  $R4$ ,  $R6$ , and  $R8$  values consistent with the uncertainties of the A1 data. The fitting function contained three free parameters ( $A$ ,  $R2$ ,  $R4$ ), while the  $R6$  and  $R8$  parameters were fixed to  $26 \text{ fm}^6$  and to  $374 \text{ fm}^8$ , respectively. The results are presented in Table 4.

Table 4 shows that the fits with a fixed  $R6$  parameter ( $R6 = 26 \text{ fm}^6$ ) reproduce  $R2$  with  $\pm 0.56 \%$  sys-



**Table 3:** The results of fitting of the  $G_E^2(Q^2)$  distribution obtained from the ratio of the differential cross sections  $d\sigma/dt(R_p = 0.8775 \text{ fm}) / d\sigma/dt(R_p = 0)$  generated with high statistics ( $N_{ev}(R_p = 0.8775 \text{ fm}) = 6.96369 \cdot 10^{10}$  events,  $N_{ev}(R_p = 0) = 7.13227 \cdot 10^{10}$  events). A polynomial form factor FF\* was used to generate  $d\sigma/dt(R_p = 0.8775 \text{ fm})$  with  $R_2$ ,  $R_4$ ,  $R_6$ , and  $R_8$  parameters (denoted by FF\*) taken from the analysis of the A1 data [5]. The generated pseudo-data were fitted with a polynomial function with various options of the fixed  $R_8$  and  $R_6$  parameters.

	$R_2 - R_2^*, fm^2$	$R_2, fm^2$	$R_4, fm^4$	$R_6, fm^6$	$R_8, fm^8$	$\chi^2/ndf$	$A$
FF*		0,7700*	2,63*	26*	374*		
FIT1	-0.0013 (6)	0.7687 (6)	2.54 (4)	22.9 (1.4)	374 fixed	963/996	1,00000 (1)
FIT2	-0.0022 (6)	0,7678 (6)	2,43 (4)	13,9 (1.4)	0,00 fixed	966/996	1,00000 (1)
FIT3	-0.0002 (3)	0,7698 (3)	2,64 (4)	30,9 (1.4)	0,00 fixed	966/996	1,00000 (1)
FIT4	-0.0002 (3)	0.7698 (3)	2,63 (1)	26 fixed	374 fixed	968/997	1,00000 (1)
FIT5	-0.0064 (3)	0,7636 (3)	2,16 (1)	10 fixed	374 fixed	1046/997	1,00000 (1)
FIT6	+0.0054 (3)	0.7753 (3)	3,03 (1)	40 fixed	374 fixed	1106/997	1,00000 (1)

tematic error ( $\pm 0.28\%$  error in the proton radius), assuming that the  $R_6$  value in the real experimental data will be in the limits  $11 fm^6 < R_6 < 41 fm^6$ .

**Table 4:** The results of fitting of the  $G_E^2(Q^2)$  distributions obtained from the ratio of the differential cross sections  $d\sigma/dt(R_p = 0.8775 \text{ fm}) / d\sigma/dt(R_p = 0)$  generated with high statistics ( $N_{ev}(R_p = 0.8775 \text{ fm}) = 6.96369 \cdot 10^{10}$  events,  $N_{ev}(R_p = 0) = 7.13227 \cdot 10^{10}$  events) with three options of the polynomial form factor, FF\*1, FF\*2, FF\*3, consistent with the uncertainties of the A1 data. The generated pseudo-data were fitted with a polynomial function  $G_E(Q^2) = A \cdot (1 - R_2 \cdot B_2 \cdot Q^2/C_2 + R_4 \cdot B_4 \cdot Q^4/C_4 - R_6 \cdot B_6 \cdot Q^6/C_6 + R_8 \cdot B_8 \cdot Q^8/C_8)$  with the  $R_6$  and  $R_8$  parameters fixed to  $26 fm^6$  and to  $374 fm^8$ , respectively. The  $A$  parameter proved to be 1.00000 with  $10^{-5}$  error in all fits.

Fit#	$R_2, fm^2$	$(R_2 - R_2^*), fm^2$	$R_4, fm^4$	$R_6, fm^6$	$R_8, fm^8$	$\chi^2/ndf$
FF*1 Fit	0.7700* 0.7699(3)	-0.0001(3)	2.63* 2.626(3)	26.0* 26 fixed	374* 374 fixed	968/997
FF*2 Fit	0.7700* 0.7742(3)	+0.0042(3)	2.43* 2.772(9)	11* 26 fixed	160* 374 fixed	1052/997
FF*3 Fit	0.7700* 0.7656(3)	-0.0044(3)	2.83* 2.482(3)	41* 26 fixed	600* 374 fixed	988/997

## 4 Summary

We have analyzed the simulated pseudo-data of the  $ep$  scattering experiment aimed at high precision measurement of the proton charge  $rms$ -radius  $R_p = \langle r_p^2 \rangle^{1/2}$ . Following the Proposal of our experiment, it was accepted that 70 million of the  $ep$  elastic scattering events will be collected in the  $Q^2$  range  $0.001 \text{ GeV}^2 \leq Q^2 \leq 0.04 \text{ GeV}^2$ . The  $ep$  elastic scattering events were generated with the polynomial proton charge form factor determined by J.C.Bernauer et al. in the data analysis of the A1 experiment [5,6], with an additional assumption that  $G_M(Q^2) = \mu_p \cdot G_E(Q^2)$  in the considered  $Q^2$  range. The generated pseudo-data were fitted with a polynomial function:

$G_E(Q^2) = A \cdot (1 - \langle r_p^2 \rangle \cdot B_2 \cdot Q^2 / C_2 + \langle r_p^4 \rangle \cdot B_4 \cdot Q^4 / C_4 - \langle r_p^6 \rangle \cdot B_6 \cdot Q^6 / C_6 + \langle r_p^8 \rangle \cdot B_8 \cdot Q^8 / C_8)$ , where  $B_n = (5.06773)^n$ ,  $C_n = (n+1)!$ ,  $n = 2, 4, 6, 8$ ;  $\langle r_p^n \rangle$  and  $Q^n$  are expressed in  $fm^n$  and in  $GeV^n$ , respectively.

Two options have been tested:

- Option 1:  $A$ ,  $\langle r_p^2 \rangle$ ,  $\langle r_p^4 \rangle$ ,  $\langle r_p^6 \rangle$  are free parameters,  $\langle r_p^8 \rangle$  is a fixed variable;
- Option 2:  $A$ ,  $\langle r_p^2 \rangle$ ,  $\langle r_p^4 \rangle$  are free parameters,  $\langle r_p^6 \rangle$  and  $\langle r_p^8 \rangle$  are fixed variables.

The results of the analysis can be summarized as follows:

- The  $Q^8$  term plays very little role in determination of  $R_p$ . The variation of  $\langle r_p^8 \rangle$  from zero to  $700 \text{ fm}^8$  leads to increasing the  $R_p$  value by  $0.001 \text{ fm}$ . Therefore, one can fix  $\langle r_p^8 \rangle$ , for example, at the value from the A1 analysis ( $\langle r_p^8 \rangle = 374 \text{ fm}^8$  [5]). This may introduce a systematic error in  $R_p$  due to uncertainties in  $\langle r_p^8 \rangle$  on a negligible level of  $\pm 0.0005 \text{ fm}$ .
- The statistical error in  $R_p$  in the fits with four free parameters ( $A$ ,  $\langle r_p^2 \rangle$ ,  $\langle r_p^4 \rangle$ ,  $\langle r_p^6 \rangle$ ) is  $\pm 0.0085 \text{ fm}$ . The advantage of such fit is a negligibly small systematic bias.
- The statistical error in  $R_p$  can be reduced by a factor of two (down to  $\pm 0.0042 \text{ fm}$ ) in the fit with three free parameters ( $A$ ,  $\langle r_p^2 \rangle$ ,  $\langle r_p^4 \rangle$ ) by fixing  $\langle r_p^6 \rangle$  to some value followed from the analysis of the  $ep$  scattering data in the higher  $Q^2$  region. However, in this case some systematic bias may be introduced because of uncertainties in the  $\langle r_p^6 \rangle$  value. The sensitivity of  $R_p$  to variations in  $\langle r_p^6 \rangle$ , as determined in our analysis, is as follows: a shift in  $\langle r_p^6 \rangle$  by  $6 \text{ fm}^6$  produces a shift in  $R_p$  by  $0.001 \text{ fm}$ .
- The existing polynomial fits to the available  $ep$  scattering data determined various moments of the proton form factor  $\langle r_p^n \rangle$  [5,6]. In particular, it was found that  $\langle r_p^6 \rangle = 29.8 (7.6)(12.6) \text{ fm}^6$ . Unfortunately, this result suffers from a large systematic error, which corresponds to a  $\pm 0.0025 \text{ fm}$  systematic bias in the extracted value of the proton radius  $R_p$ .
- Another approach to the proton form factor was demonstrated recently by J.M. Alarcon et al. [7,8]. On the basis of the Dispersive Improved Chiral Effective Field Theory, they calculated various FF moments from  $\langle r_p^2 \rangle$  to  $\langle r_p^{20} \rangle$  with remarkably small error bars. Their predictions for the lowest moments of the charge FF are:  $\langle r_p^2 \rangle = (0.701, 0.768) \text{ fm}^2$ ,  $\langle r_p^4 \rangle = (1.47, 1.60) \text{ fm}^4$ ,  $\langle r_p^6 \rangle = (8.5, 9.0) \text{ fm}^6$ ,  $\langle r_p^8 \rangle = (127, 130) \text{ fm}^8$ . Note that precision of the calculations is higher for higher FF moments in this approach, so it looks safe to take the predicted values of  $\langle r_p^6 \rangle = 9.0 \text{ fm}^6$  and  $\langle r_p^8 \rangle = 130 \text{ fm}^8$  for our fits. The systematic bias will be negligible in this case, even assuming the real error in  $\langle r_p^6 \rangle$  will be an order of magnitude larger than that quoted above.
- Besides the proton radius  $R_p$ , the  $\langle r_p^4 \rangle$  parameter will be also determined with 8% statistical errors in the fits with fixed  $\langle r_p^6 \rangle$  and  $\langle r_p^8 \rangle$ .

In conclusion, Table 5 presents the statistical and systematic errors related to the procedure of extraction of the proton charge radius from the experimental data expected in our experiment.

**Table 5:** Statistical and systematic errors in  $R_p$  resulted in the fits of the psuedo-data with a polynomilal function  $G_E(Q^2) = A \cdot (1 - \langle r_p^2 \rangle \cdot B_2 \cdot Q^2 / C_2 + \langle r_p^4 \rangle \cdot B_4 \cdot Q^4 / C_4 - \langle r_p^6 \rangle \cdot B_6 \cdot Q^6 / C_6 + \langle r_p^8 \rangle \cdot B_8 \cdot Q^8 / C_8)$  with three or four free parameters. Statistics :  $7 \cdot 10^7 ep$  scattering events in the  $Q^2$  range  $0.001 \text{ GeV}^2 \leq Q^2 \leq 0.04 \text{ GeV}^2$ .

	Free parameters	Fixed parameters	$\Delta R_p$ (stat)	$\Delta R_p$ (syst)	comments
<b>Option1</b>	$A \langle r_p^2 \rangle < r_p^4 \rangle < r_p^6 \rangle$	$\langle r_p^8 \rangle$	$\pm 0.0085 \text{ fm}$	$< 0.001 \text{ fm}$	---
<b>Option2</b>	$A \langle r_p^2 \rangle < r_p^4 \rangle$	$\langle r_p^6 \rangle < r_p^8 \rangle$	$\pm 0.0042 \text{ fm}$	$\pm 0.0025 \text{ fm}$ $< 0.001 \text{ fm}$	$\langle r_p^6 \rangle$ from[6] $\langle r_p^8 \rangle$ from[7]

Some other options of the analysis are presented in the ANNEXes to this note.

## References

1. J. Bernauer et al. (A1 Collaboration), Phys. Rev. Lett. 105, 242001 (2010).
2. A. Antognini et al., Science **339**, 417 (2013).
3. Conference at Trento, June 2016. <http://www.ectstar.eu/node/1659>.
4. A. Vorobyev, et.al, Proposal to perform an experiment at the A2 hall, MAMI, November 2017. "High Precision Measurement of the ep elastic cross section at small  $Q^2$ ".
5. J. C. Bernauer, Ph.D. thesis, University of Mainz, 2010.
6. M. O. Distler, J. C. Bernauer, and T. Walcher Phys. Lett.
7. J.M. Alarcon, C. Weiss ArXiv: 1803.09748 [hep-ph] Phys.Lett.B 784 (2018) 373.
8. J.M. Alarcon et al. ArXiv: 1809.06373 [hep-ph].

## Annex 1. Fits with fixed ratio $\eta = R6/R4$

The parameter  $R6$  is rather strongly correlated with  $R4$  as it can be seen from Table 6.

**Table 6:** The values of  $R4$  and  $R6$  in different presentations of the proton Form Factor, corresponding to  $R2 = 0.7700 \text{ fm}^2$

Form Factor	$R4, \text{fm}^4$	$R6, \text{fm}^6$	$\eta = R6/R4, \text{fm}^2$
Dipole FF	1.49	5.3	3.6
$\text{Di}\chi\text{EFT}$ [7,8]	1.6	9.0	5.6
Bernauer [5]	2.63	26	9.9

Therefore, instead of  $R6$ , one can try to use in the fitting function the ratio  $\eta = R6/R4$ . That is, instead of eq.( 7), to use the following expression in the fits:

$$G_E(Q^2)_{fit} = A \cdot (1 - R2 \cdot B_2 \cdot Q^2/C_2 + R4 \cdot B_4 \cdot Q^4/C_4 - \eta \cdot R4 \cdot B_6 \cdot Q^6/C_6 + R8 \cdot B_8 \cdot Q^8/C_8) \quad (8)$$

where  $\eta$  is a variable parameter. This fitting function was used to fit the psedo-data generated with the Bernauer's Form Factor, following the procedure described above in this note. The value of  $\eta$  was varied from  $\eta=6$  to  $\eta=12$ , with  $R8 = 374 \text{ fm}^8$ . The fitting procedure is illustrated by Fig. 8 which shows the distribution of the fit parameters  $A$ ,  $R2$ ,  $R4$ , and  $\chi^2/\text{ndf}$  obtained in the fits with the regular statistics (panels a), b), c), d)). Also, this Figure (panel e)) shows an example of the super high statistics fit used for studies of the systematic shifts in the measured values of  $R2$  and  $R4$  in dependence on the value of the ratio  $\eta$ . The results of these studies are presented in Table 7.

**Table 7:** The results of fitting the ratio of the differential cross sections  $d\sigma/dt(R_p = 0.8775 \text{ fm}) / d\sigma/dt(R_p = 0)$  generated with the Bernauer's Form Factor FF\*. The generated pseudo - data were fitted with a polynomial function  $G_E(Q^2) = A \cdot (1 - R2 \cdot B_2 \cdot Q^2/C_2 + R4 \cdot B_4 \cdot Q^4/C_4 - \eta \cdot R4 \cdot B_6 \cdot Q^6/C_6 + R8 \cdot B_8 \cdot Q^8/C_8)$  ( $R_p = 0.8775 \text{ fm}$ ) =  $6.96369 \cdot 10^{10}$  events. Binning: 1000 bins

Fit#	$R2, \text{fm}^2$	$R2 - R2^*, \text{fm}^2$	$R4, \text{fm}^4$	$R6/R4, \text{fm}^2$	$R8, \text{fm}^8$	$\chi^2/\text{ndf}$
FF*	0.7700*		2.63*	9.9*	374*	
Fit 1	0.7651(3)	- 0.0049(3)	1.33(1)	6 fixed	374 fixed	992/997
Fit 2	0.7674(3)	- 0.0026(3)	1.48(1)	8 fixed	374 fixed	975/997
Fit 3	0.7700(3)	0.0000(3)	1.62(1)	10 fixed	374 fixed	953/997
Fit 4	0.7729(3)	+ 0.0029(3)	1.91(1)	12 fixed	374 fixed	1010/997

As it follows from Table 7, the variation of the ratio  $R6/R4$  from  $6 \text{ fm}^2$  to  $12 \text{ fm}^2$  resulted in a 1% shift in the value of  $R2$  ( 0.5% shift in  $R_p$ ).

In other words, with the ratio  $R6/R4$  fixed to  $8 \text{ fm}^2$ , one can expect a systematic bias in the measured *rms*-proton radius  $\Delta R_p = \pm 0.0014 \text{ fm}$ , assuming that in the real experimental data this ratio will be between  $6 \text{ fm}^2$  (  $\text{Di}\chi\text{EFT}$ ) and  $10 \text{ fm}^2$  (Bernauer).

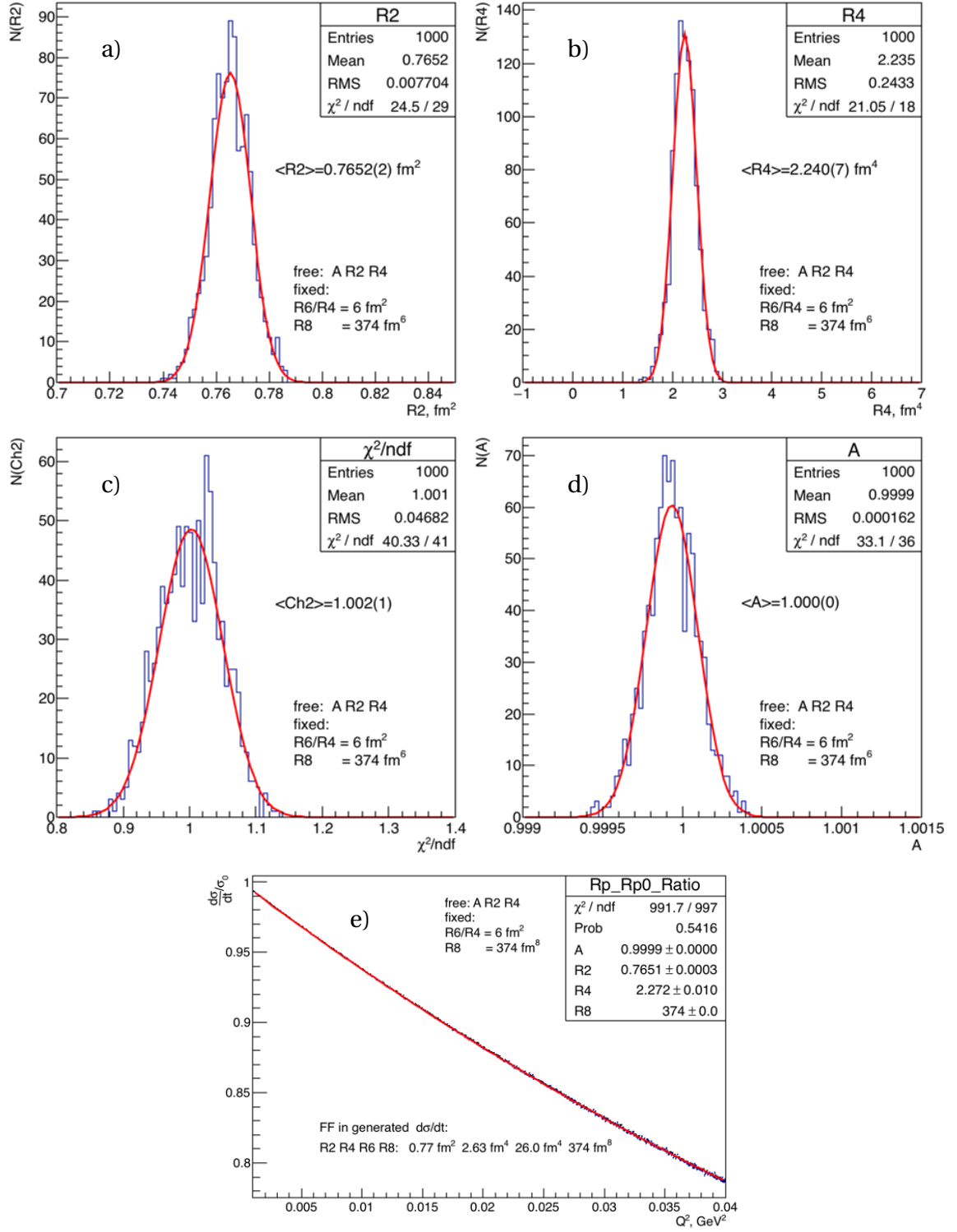


**Figure 8:**

**Panels a) b) c) d).** Distribution of the fit parameters obtained from 1000 independent fits of  $d\sigma/dt$  generated in the  $Q^2$  range from  $0.001 \text{ GeV}^2$  to  $0.04 \text{ GeV}^2$  using Bernauer's proton form factor. *Statistics:*  $7 \cdot 10^7$  events in each generated set. *Binning:* 1000 bins. Fitting with binomial FF containing up to  $Q^8$  term. *Free parameters:*  $A, R2, R4$ . *Fixed parameters:*  $R8 = 374 \text{ fm}^8$  and  $R6/R4 = 6 \text{ fm}^2$ .

**Panel e).** Results of one fitting set with super high statistics :  $7 \cdot 10^9$  events. All fit conditions are as above.

## Annex 2. Dipole Form Factor

Similar analysis was performed using a modified Dipole Form Factor in the generated differential cross section  $d\sigma/dt$  :

$$G_E(Q^2) = (1 + Q^2/0.6068)^{-2}.$$

The power series expansion of this form factor corresponds to the following parameters:

$$\langle r_p^2 \rangle = 0.7700 \text{ fm}^2, \langle r_p^4 \rangle = 1.49 \text{ fm}^4, \langle r_p^6 \rangle = 5.3 \text{ fm}^6, R_p = \langle r_p^2 \rangle^{1/2} = 0.8775 \text{ fm}.$$

The cross sections integrated over the  $Q^2$  range  $0.001 \text{ GeV}^2 \leq Q^2 \leq 0.04 \text{ GeV}^2$  is :

$$\sigma(R_p = 0.8775 \text{ fm}) = 0.248604 \text{ mb}.$$

The ratio of the cross sections is:

$$\eta = \sigma(R_p = 0.8775 \text{ fm}) / \sigma(R_p = 0) = 0.975974.$$

Fig.9 shows the ratio of the cross sections  $d\sigma/dt(R_p = 0.8775 \text{ fm}) / d\sigma/dt(R_p = 0)$  generated with the modified Dipole Form Factor. Table 8 presents the results of the fits of this ratio using a polynomial  $G_E = A(1 - R_2Q^2 + R_4Q^4 - R_6Q^6 + R_8Q^8)$  with fixed parameters  $R_6$  and  $R_8$ .

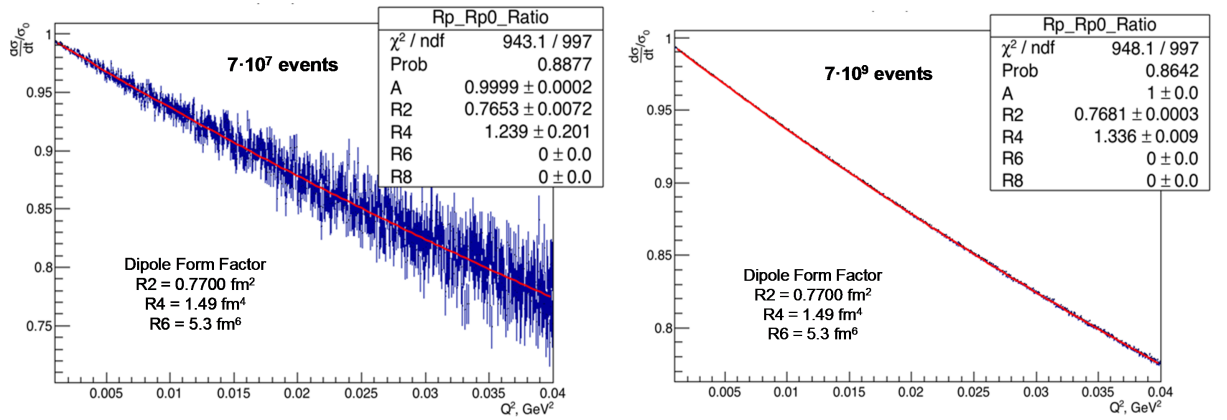


**Figure 9:** Distribution of the ratio  $d\sigma/dt(R_p = 0.8775 \text{ fm}) / d\sigma/dt(R_p = 0)$  generated with a modified Dipole Form Factor. Statistics:  $N_{ev}(R_p = 0.8775 \text{ fm}) = 6.9636 \cdot 10^7$  events (left panel),  $N_{ev}(R_p = 0.8775 \text{ fm}) = 6.96369 \cdot 10^9$  events (right panel). Binning: 1000 bins. Red lines show the results of the fit with the form factor represented by Fit 1 in Table 8

**Table 8:** The results of fitting the ratio of the differential cross sections  $d\sigma/dt(R_p = 0.8775 \text{ fm}) / d\sigma/dt(R_p = 0)$  generated with the modified Dipole Form Factor. The generated pseudo - data were fitted with a polynomial function  $G_E(Q^2) = A \cdot (1 - R_2 \cdot B_2 \cdot Q^2/C_2 + R_4 \cdot B_4 \cdot Q^4/C_4 - \eta \cdot R_4 \cdot B_6 \cdot Q^6/C_6 + R_8 \cdot B_8 \cdot Q^8/C_8)$  with  $R_8 = 0$  and various values of fixed  $R_6$ . Statistics:  $N_{ev}(R_p = 0.8775 \text{ fm}) = 6.96369 \cdot 10^{10}$  events. Binning: 1000 bins.

Fit#	$R_2, \text{fm}^2$	$R_2 - R_2^*, \text{fm}^2$	$R_4, \text{fm}^4$	$R_6/R_4, \text{fm}^2$	$R_8, \text{fm}^8$	$\chi^2/ndf$
FF*	0.7700*		1.49*	5.3*		
Fit 1	0.7681(3)	- 0.0019(3)	1.33(1)	0 fixed	0 fixed	948/997
Fit 2	0.7700(3)	0.0000(3)	1.48(1)	5 fixed	0 fixed	952/997
Fit 3	0.7720(3)	+ 0.0020(3)	1.62(1)	10 fixed	0 fixed	980/997
Fit 4	0.7759(3)	+ 0.0041(3)	1.91(1)	20 fixed	0 fixed	1110/997

**As it follows from Table Table 8, the variation of  $R_6$  in the fitting function from  $R_6 = 0$  to  $R_6 = 10 \text{ fm}^6$  resulted in a systematic shift in the extracted value of  $R_2$  by 0.5% (0.25% in  $R_p$ ).**